PROCEEDINGS OF SCIENCE

Pion electromagnetic form factor from full lattice QCD

Jonna Koponen*
SUPA, School of Physics and Astronomy, University of Glasgow, Glasgow, G12 8QQ, UK
E-mail: jonna.koponen@glasgow.ac.uk

Francis Bursa

SUPA, School of Physics and Astronomy, University of Glasgow, Glasgow, G12 8QQ, UK

Christine T. H. Davies

SUPA, School of Physics and Astronomy, University of Glasgow, Glasgow, G12 8QQ, UK

Rachel J. Dowdall

DAMTP, University of Cambridge, Wilberforce Road, Cambridge, CB3 0WA, UK

G. Peter Lepage

Laboratory of Elementary-Particle Physics, Cornell University, Ithaca, New York 14853, USA

We present the first calculation of the pion electromagnetic form factor at physical light quark masses. This form factor parameterises the deviations from the behaviour of a point-like particle when a photon hits the pion. These deviations result from the internal structure of the pion and can thus be calculated in QCD. We use three sets (different lattice spacings) of $n_f = 2+1+1$ lattice configurations generated by the MILC collaboration. The Highly Improved Staggered Quark formalism (HISQ) is used for all of the sea and valence quarks. Using lattice configurations with *u*/*d* quark masses very close to the physical value is a big advantage, as we avoid the chiral extrapolation. We study the shape of the vector (f_+) form factor in the q^2 range from 0 to -0.15 GeV^2 and extract the mean square radius, $\langle r_v^2 \rangle$. The shape of the vector form factor and the resulting radius is compared with experiment. We also discuss the scalar form factor and radius extracted from that, which is not directly accessible to experiment. We have also calculated the contributions from the disconnected diagrams to the scalar form factor at small q^2 and discuss their impact on the scalar radius $\langle r_s^2 \rangle$.

The 33rd International Symposium on Lattice Field Theory
14 -18 July 2015
Kobe International Conference Center, Kobe, Japan

*Speaker.

PoS(LATTICE 2015)119

1. Introduction

When a photon hits a π meson it sees the internal structure of the π i.e. its quark constituents and their strong interaction. The electromagnetic form factor of the pion parameterises these deviations from the behaviour of a point-like particle. The form factor can be calculated in QCD but a fully nonperturbative treatment (e.g. lattice QCD) is necessary. The NA7 Collaboration have determined the vector form factor directly experimentally from $\pi - e$ scattering [1] in a model-independent way. Here we concentrate on calculating the form factor at small (negative) values of 4-momentum transfer, q^2, as the experimental error is 1-1.5% in the region up to $|q^2| = 0.1$ GeV^2 and so a lattice QCD calculation of the form factor there can provide a stringent test of QCD.

In the nonrelativistic limit, where $q^2 \approx -(\vec{q})^2$, the electromagnetic (i.e. vector) form factor, $f_+(q^2)$, can be viewed as the Fourier transform of the electric charge distribution. The mean squared radius obtained by integrating over this distribution is then given by

$$\langle r^2 \rangle = 6 \frac{df_+(q^2)}{dq^2}\bigg|_{q^2=0}. \tag{1.1}$$

This is adopted more generally as a definition of $\langle r^2 \rangle$, since it is useful to have a single number with which to characterise the shape of the form factor. We will use it here to compare different lattice calculations and also to compare lattice results against experiment.

2. Lattice calculation

Calculating the $\langle r^2 \rangle$ in lattice QCD is challenging as the result is very sensitive to the mass of the π. It has been numerically too expensive until recently to include u/d quarks with their physically very light masses in lattice QCD calculations: The lightest π meson mass used in earlier calculations of the electromagnetic form factor has been in the range of 250-400 MeV, and results have had to be extrapolated to the physical point using chiral perturbation theory.

Here we give results for both vector and scalar form factors for π mesons made of physical u/d quarks and including a fully realistic quark content in the sea, with physical u, d, s and c quarks. We use lattice ensembles provided by the MILC Collaboration [2, 3], which allows us also to work with three different values of the lattice spacing — the lattice parameters are listed in Table 2. This enables good control of systematic errors both from m_π and from discretisation. The ensembles we use have large volumes with a minimum spatial size of 4.8 fm.

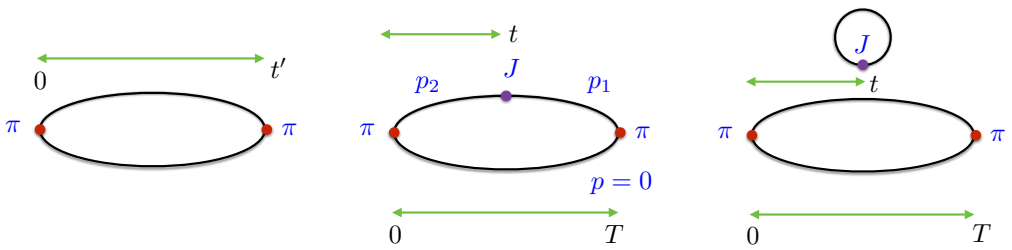

Figure 1: 2-point (left) and 3-point quark-line-connected (middle) and quark-line-disconnected (right) correlators.

Set	a/fm	$am_{\ell,sea}$	$am_{s,sea}$	$am_{c,sea}$	$L_s \times L_t$	$n_{\rm cfg}$	T
1	0.1509	0.00235	0.0647	0.831	32×48	1000	9,12,15
2	0.1212	0.00184	0.0507	0.628	48×64	1000	12,15,18
3	0.0879	0.0012	0.0363	0.432	64×96	223	16,21,26

Table 1: The MILC gluon field ensembles used here [2, 3]. Set 1 will be referred to "very coarse", 2 as "coarse" and 3 as "fine". The second column gives the lattice spacing (determined in [4]). Columns 3, 4 and 5 give the sea quark masses ($m_u = m_d = m_\ell$). L_s and L_t are the lengths in lattice units in space and time directions for each lattice. The number of configurations that we have used in each set is given in the seventh column. The 8th column gives the values of the end-point of the 3-point function, T, in lattice units.

We use the same action (HISQ) and same light quark masses for the valence quarks as for the sea quarks, and combine the light quark propagators into 2-point and 3-point correlators as illustrated in Fig. 1. We consider two currents J, a vector current and a scalar current. When J is a vector current we need to consider only one 3-point diagram, the quark-line connected diagram shown as the central diagram of Fig. 1. The quark-line disconnected diagram (on the right in Fig. 1.) vanishes for vector current in the ensemble average because it is odd under charge-conjugation, but for scalar J it needs to be included. We use twisted boundary conditions [5] to give one or two of the quarks spatial momentum, which allows us to obtain the form factors at different values of q^2. More details of the calculation can be found in [6].

3. Electromagnetic form factor

To extract the form factor we fit all sets of 2-point and 3-point correlators (at various values of spatial momenta p_1 and p_2) on a given ensemble simultaneously. We use a multi-exponential fit and Bayesian methods that allow us to include the effect of excited states [6].

We can then relate the ground state amplitude of the 3-point correlator from the fit, $J_{0,0}$, to the matrix element between the ground state mesons and further to the electromagnetic form factor by

$$f_+(q^2)(p_1+p_2)_i = \langle \pi(p_1)|V_i|\pi(p_2)\rangle = Z\sqrt{4E_0(p_1)E_0(p_2)}J_{0,0}(p_1,p_2), \tag{3.1}$$

where $E_0(p)$ is the ground state energy of the meson with momentum p. We determine Z, the renormalisation factor, by using the fact that $f_+(0) = 1$ for a conserved current.

Our results for the electromagnetic form factor f_+ are plotted against q^2 in Fig. 2 for all three sets along with the results from experiment [1]. The agreement is very good, reflecting the fact that our results correspond to physical π masses.

In fitting a functional form in q^2 to our results to extract a mean squared radius, we use the same monopole form as that used for the experimental results [1], but including allowance for finite lattice spacing effects and slight mistuning of sea quark masses [6]. We also include a logarithmic term in m_π^2 to make small adjustments for the fact that our u/d quark masses are not exactly at their physical values (in fact they are slightly too low). We plot the result of the fit in Fig. 2 alongside with our raw data and experimental results. Our final result for the mean square charge radius is $\langle r^2\rangle_V^{(\pi)} = 0.403(18)(6)$ fm^2, where the first error is from fitting/statistics and the second error includes all systematic uncertainties. More details of the fit and a full error budget can be found in [6].

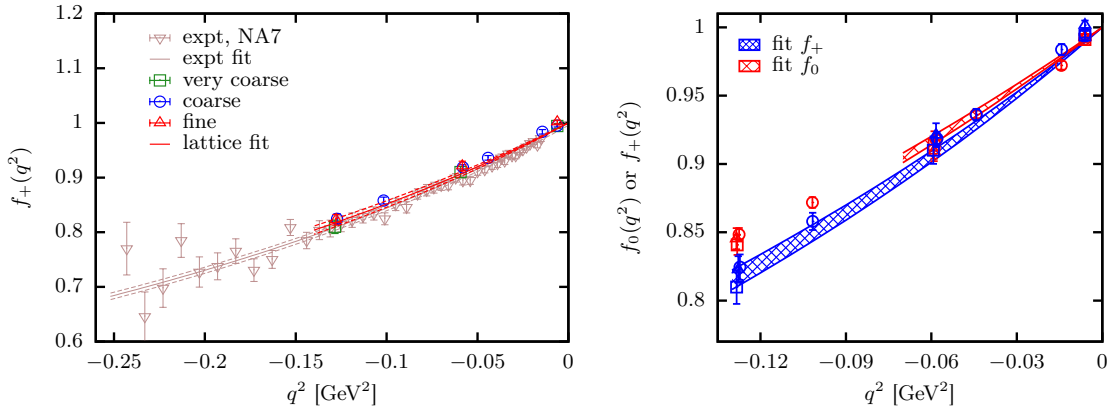

Figure 2: On the left: Lattice QCD results for the vector form factor on each ensemble compared directly to the experimental results from [1]. Fit curves for both experiment and lattice QCD results are given to a 'monopole' form. On the right: Comparison of our lattice QCD results for the pion vector form factor (blue) with the connected part of the pion scalar form factor (red). Results from set 1 are shown as open squares, set 2 as circles and set 3 as triangles. The hashed curves give the fit to the form factors described in the text.

4. Scalar form factor

The calculation for the connected scalar form factor proceeds in an identical way to that of the vector form factor. The ground-state matrix element for the scalar current is related to the parameter $J_{0,0}$ extracted from our fits as in eq. (3.1). In turn the matrix element is related to the form factor that we wish to extract by

$$\langle \pi(p_1)|S|\pi(p_2)\rangle^{\text{conn}} = A f_0^{\text{conn}}(q^2), \tag{4.1}$$

where A is a normalisation factor. If we had included disconnected diagrams we would be able to write, from the Feynman-Hellmann theorem,

$$\langle \pi(p_1)|S|\pi(p_2)\rangle = f_0(q^2)\frac{\partial M_\pi^2}{2\partial m_\ell}, \tag{4.2}$$

with $f_0(0) = 1$ (our scalar current is absolutely normalised). Since here we are chiefly concerned with the shape of the form factor, we simply treat the scalar current as requiring a normalisation factor, Z_S, and determine this from the requirement that also $f_0(0) = 1$.

To determine the mean squared radius associated with the connected scalar form factor we take the same fit as for the vector case, except that the coefficient of the chiral logarithm is now larger. Our final result is $\langle r^2\rangle^{(\pi)}_{S,\text{conn}} = 0.349(18)(36)$ fm^2. This radius has a central value that is only slightly smaller than the vector form factor radius as illustrated in Fig. 2.

For the full scalar form factor we need to include the quark-line disconnected contribution illustrated in Fig. 1. We can then define flavour-singlet and flavour-octet scalar currents:

$$S_{\text{singlet}} = 2\bar{\ell}\ell + \bar{s}s \quad \text{and} \quad S_{\text{octet}} = 2\bar{\ell}\ell - 2\bar{s}s. \tag{4.3}$$

Scalar form factors for these two currents are then determined by combining the connected scalar form factor with disconnected contributions in appropriate combinations from quark loops made from ℓ quarks or s quarks.

For the $q^2 = 0$ case it is relatively simple to calculate the disconnected contributions: for the $\bar{s}s$ scalar current this is the π meson equivalent of the 'strangeness in the nucleon' calculation. The disconnected contribution for current $\bar{q}q$ is

$$\langle \pi | S_{\bar{q}q} | \pi \rangle^{\text{disc}} = \langle \pi(p) | \bar{q}q | \pi(p) \rangle - \langle \pi(p) | \pi(p) \rangle \langle \bar{q}q \rangle. \tag{4.4}$$

This is determined from the correlation of a pion 2-point function with source at time 0 and sink at time T with a scalar current (condensate) summed over the timeslice at t. The second term subtracts the product of the vacuum expectation values of the π meson correlator and the condensate.

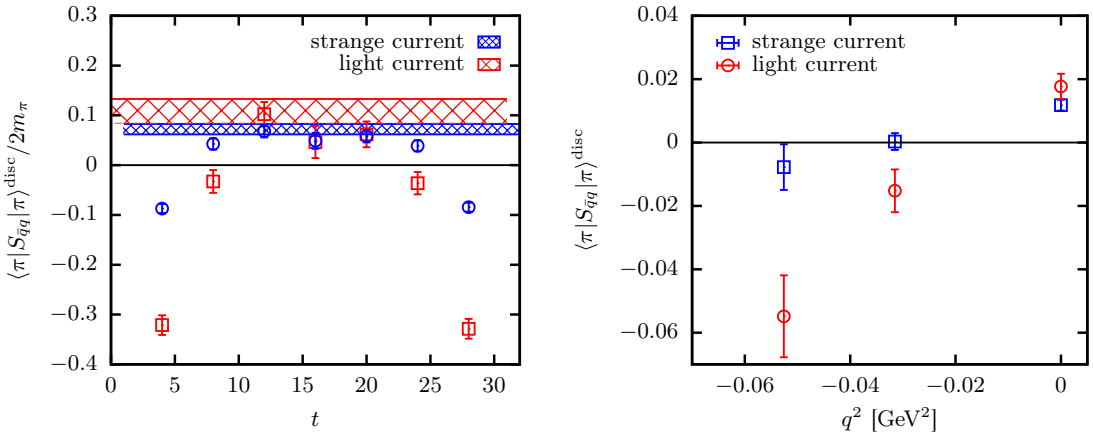

Figure 3: On the left: The ratio of 3-point correlator to 2-point correlator for the disconnected contribution for the $\ell\bar{\ell}$ (red circles) and $s\bar{s}$ currents (blue squares) to the scalar form factor of the π at $q^2 = 0$ on coarse lattices, set 2. The points are the lattice QCD results with statistical errors and the red and blue hashed bands show the ground-state fit result for the $\ell\bar{\ell}$ and $s\bar{s}$ contributions, respectively. On the right: The $s\bar{s}$ and $\ell\bar{\ell}$ disconnected contributions to the scalar form factor as a function of q^2 for coarse lattices, set 2.

The quantities required to calculate the disconnected contribution for the $s\bar{s}$ current to the scalar form factor at $q^2 = 0$ are then simply the π meson and η_s meson (the pseudoscalar $s\bar{s}$ meson) correlators. The $\bar{s}s$ current loop at time t is obtained by summing over η_s correlators with time-source t. The 3-point function that yields $\langle \pi | S_{\bar{s}s} | \pi \rangle$ of eq. (4.4) at $q^2 = 0$ is thus given by

$$C_{3pt}(p,p,0,t,T) = -\left\langle C_\pi(p,0,T) am_s \sum_{t'} C_{\eta_s}(p,t,t') \right\rangle + \left\langle C_\pi(p,0,T) \right\rangle \left\langle am_s \sum_{t'} C_{\eta_s}(p,t,t') \right\rangle \tag{4.5}$$

where $p = 0$ and the average is over gluon configurations. For the scalar current made of light quarks an equivalent expression holds, using two π meson correlators with offset time-sources. The contribution from the disconnected diagram is small, at the 1% level, compared to the connected diagram at $q^2 = 0$. Here we work only on coarse set 2.

To obtain results for the disconnected contribution to the scalar form factor at non-zero values of q^2 we need to project onto non-zero lattice spatial momenta, $2\pi/L_s(n_x, n_y, n_z)$, at T and t in the correlators used in eq. (4.5). The statistical errors grow as spatial momentum is introduced so we restrict ourselves to the smallest non-zero lattice momenta with (n_x, n_y, n_z) equal to $(1,0,0)$ and $(1,1,0)$ and permutations thereof. Our results for the disconnected diagram for both light and strange currents at $q^2 = 0$ and as a function of q^2 are plotted in Fig. 3.

To obtain the mean-square radius for the singlet and octet scalar form factors we must combine the connected and disconnected contributions. We simply add the contribution from the disconnected pieces on top of the connected results using the smallest non-zero $|q^2|$:

$$\frac{|q^2|}{6}\langle r^2\rangle = \frac{|q^2|}{6}\langle r^2\rangle^{\text{conn}}\left(1+\frac{f_0^{\text{disc}}(0)}{f_0^{\text{conn}}(0)}\right)^{-1} + \frac{f_0^{\text{disc}}(0)-f_0^{\text{disc}}(q^2)}{f_0^{\text{conn}}(0)}\left(1+\frac{f_0^{\text{disc}}(0)}{f_0^{\text{conn}}(0)}\right)^{-1}. \quad (4.6)$$

We find $\langle r^2\rangle^{(\pi)}_{S,\text{singlet}} = 0.506(38)(53)$ fm^2 and $\langle r^2\rangle^{(\pi)}_{S,\text{octet}} = 0.431(38)(46)$ fm^2. Here the first error is statistical and and the second error is systematic — see [6] for the full error budget.

5. Discussion

Figure 4 compares results presented here for the mean square of the pion charge radius to other lattice QCD calculations and to experimental results. There is also a recent calculation by B. Owen *et. al.* [7], but as there is no chiral or continuum extrapolation their results are not included in the figure. Lattice QCD results for the mean square of the pion scalar radius are summmarized in Fig. 4 on the right. The scalar form factor is not directly accessible in experiment so we compare the lattice results to a phenomenological result from $\pi-\pi$ scattering [8] and to chiral perturbation theory results for F_π/F [9] and F_K/F_π [10]. Note that adding the disconnected diagram changes the scalar radius significantly even though the contribution to the form factor is small.

Acknowledgements. We are grateful to MILC for the use of their gauge configurations and code. This work was funded by STFC, NSF, the Royal Society and the Wolfson Foundation. We used the Darwin Supercomputer of the University of Cambridge HPC Service as part of STFC's DiRAC facility. We are grateful to the Darwin support staff for assistance.

References

[1] NA7 Collaboration; S. R. Amendolia *et al.*, Nucl. Phys. B277 (1986) 168

[2] MILC Collaboration; A. Bazavov *et al.*, Phys. Rev. D82 (2010) 074501, arXiv:1004.0342

[3] A. Bazavov *et al.*, Phys. Rev. D87 (2013) 054505, arXiv:1212.4768

[4] S. Borsanyi *et al.*, JHEP 09 (2012) 010, arXiv:1203.4469

[5] D. Guadagnoli *et al.*, Phys. Rev. D73 (2006) 114504, arXiv:hep-lat/0512020

[6] HPQCD Collaboration; J. Koponen *et al.*, arXiv:1511.07382

[7] B. Owen *et al.*, Phys. Rev. D91 (2015) 074503, arXiv:1501.02561

[8] J. Gasser and H. Leutwyler, Annals Phys. 158 (1984) 142

[9] S. Aoki et al., Eur. Phys. J. C74 (2014) 2890, arXiv:1310.8555

[10] J. Gasser and H. Leutwyler, Nucl. Phys. B250 (1985) 517

[11] RBC/UKQCD collaboration; P. A. Boyle *et al.*, JHEP 0807 (2008) 112, arXiv:0804.3971

[12] PACS-CS Collaboration; O. Nguyen *et al.*, JHEP04 (2011) 122, arXiv:1102.3652

[13] JLQCD Collaboration; S. Aoki *et al.*, arXiv:1510.06470

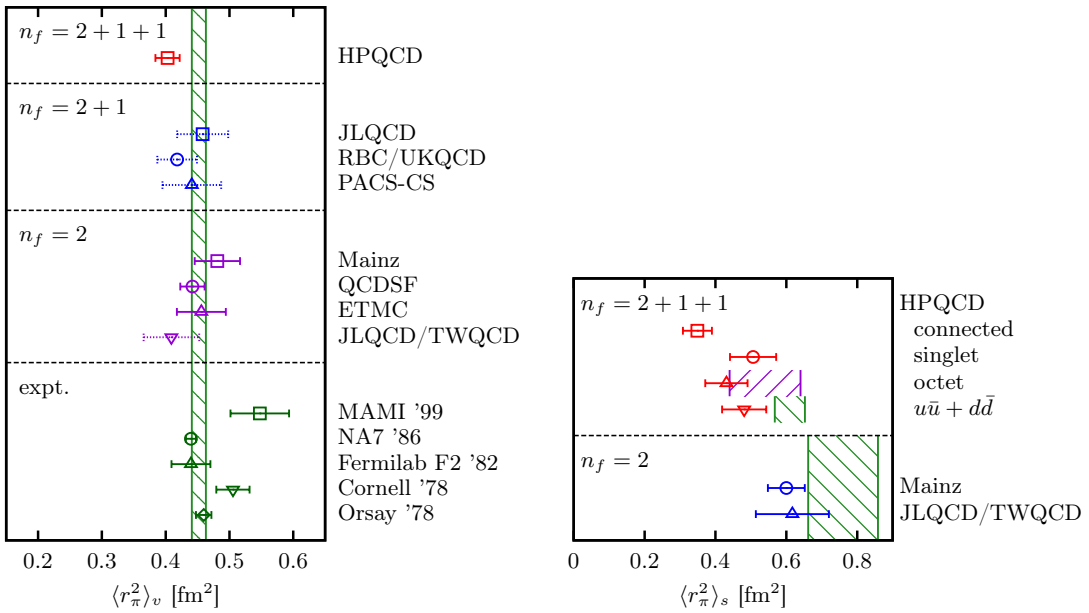

Figure 4: On the left: A summary of lattice QCD results for the mean square electric charge radius. The top result is the one presented in this paper; the $n_f = 2+1$ results are from [11, 12, 13]; and the $n_f = 2$ results are from [14, 15, 16, 17]. Results that include only one value of the lattice spacing have dotted error bars. Experimental results are from [18, 1, 19, 20, 21]. The hashed vertical line gives the average from the Particle Data Group [22]. On the right: A summary of lattice QCD results for the mean square scalar radius. The HPQCD Collaboration's results are from this paper: "connected" shows the mean square radius from the quark-line connected calculation only; "singlet" and "octet" are full calculations including quark-line disconnected diagrams arranged in flavour-singlet or flavour-octet currents (Eq. 4.3); for comparison, $u\bar{u}+d\bar{d}$ includes only u/d quarks in the scalar current. The results including only u and d quarks in the sea ($n_f = 2$) are from [23, 17]. The hashed green vertical bands give the result expected from chiral perturbation theory for F_π/F [9] for $n_f = 2$ and $n_f = 2+1$ (for comparison with our $n_f = 2+1+1$ results). The phenomenological result from $\pi-\pi$ scattering [8] is very similar to the $n_f = 2+1$ green band. The hashed purple band gives the chiral perturbation theory expectation for the scalar octet case [10].

[14] B. B. Brandt, A. Jüttner and H. Wittig, JHEP11 (2013) 034, arXiv:1306.2916

[15] QCDSF/UKQCD Collaboration; D. Brömmel *et al.*, Eur. Phys. J. C51 (2007) 335, arXiv:hep-lat/0608021

[16] ETMC; R. Frezzotti *et al.*, Phys. Rev. D79 (2009) 074506, arXiv:0812.4042

[17] JLQCD/TWQCD Collaboration; S. Aoki *et al.*, Phys. Rev. D80 (2009) 034508, arXiv:0905.2465

[18] A1 Collaboration; A. Liesenfeld *et al.* Phys. Lett B468 (1999) 20, arXiv:nucl-ex/9911003

[19] A. Quenzer *et al.*, Phys. Lett. B76 (1978) 512

[20] E. B. Dally *et al.*, Phys. Rev. Lett. 48 (1982) 375

[21] C. J. Bebek *et al.*, Phys. Rev. D17 (1978) 1693

[22] Particle Data Group; K. A. Olive *et al.*, Chin. Phys. C38 (2014) 090001

[23] V. Gülpers, G. von Hippel and H. Wittig, arXiv:1507.01749